Psychopharmacology (2022) 239:365–376
https://doi.org/10.1007/s00213-021-05998-2

ORIGINAL INVESTIGATION

Mapping the effects of atomoxetine during response inhibition across cortical territories and the locus coeruleus

Rong Ye[1,2] · Ndabezinhle Mazibuko[2] · Jens Teichert[3] · Ralf Regenthal[3] · Angie A. Kehagia[2,4] · Mitul A. Mehta[2]

Received: 3 May 2021 / Accepted: 4 October 2021 / Published online: 25 October 2021

Abstract

Rationale The effects of atomoxetine (ATO) on response inhibition have been typically examined using the stop signal task (SST) which is however confounded by attentional capture. The right inferior frontal cortex (rIFC) has been implicated in the modulation of ATO on inhibitory control, but a precise characterisation of its role is complicated by its functional inhomogeneity.

Objectives The current study aimed to directly investigate the effect of ATO in the SST using the imaging contrast unconfounded by attentional capture, to test the specific drug actions in functionally dissociable rIFC subregions, and to explore the role of locus coeruleus (LC), the main source of cortical noradrenaline, in mediating the drug effects.

Methods This imaging study investigated the effect of ATO (40 mg) in 18 human participants during a modified SST that unconfounds attention from inhibition. Functional definitions for rIFC subdivisions were adopted in the analyses to isolate attention and inhibition during action cancellation. The LC integrity was measured in vivo using a neuromelanin-sensitive sequence.

Results We identified one mechanism of ATO modulation specific to inhibitory control: ATO enhanced activity in pre-supplementary area (pre-SMA) for motor inhibition, and the recruitment of temporoparietal junction (TPJ) and inferior frontal junction (IFJ) for functional integration during response inhibition. Moreover, drug-related behavioural and neural responses correlated with variations in LC integrity.

Conclusions These findings provide a more nuanced and precise understanding of the effects of ATO on specific and domain general aspects of stopping.

Keywords Atomoxetine · Functional magnetic resonance imaging · Locus coeruleus · Response inhibition · Stop signal task

Introduction

The ability to inhibit undesirable actions upon the presentation of a stop signal can be indexed using response inhibition paradigms such as the stop signal task (SST). SST variants have been used to index inhibitory control in neuropsychiatric conditions (Dalley and Robbins 2017; Gilmour et al. 2013; Lipszyc and Schachar 2010; Verbruggen and Logan 2008) and healthy ageing (Coxon et al. 2016; Sebastian et al. 2013; Tsvetanov et al. 2018). A single dose of atomoxetine (ATO), which increases extracellular levels of dopamine and noradrenaline (Bymaster et al. 2002), modulates SST performance in experimental animals (Bari et al. 2009; Robinson et al. 2008), healthy human subjects (Chamberlain et al. 2006) and patients with Parkinson's disease (PD) (Kehagia et al. 2014) and attention deficit hyperactivity disorder

✉ Rong Ye
ronye.uk@gmail.com

1 Department of Clinical Neurosciences and Cambridge University Hospital NHS Trust, University of Cambridge, Herchel Smith Building, Robinson Way, Cambridge CB2 0SZ, UK

2 Centre for Neuroimaging Sciences, Institute of Psychiatry, Psychology and Neuroscience, King's College London, London, UK

3 Division of Clinical Pharmacology, Rudolf-Boehm-Institute of Pharmacology and Toxicology, Leipzig University, Leipzig, Germany

4 University College Hospital, University College London Hospitals NHS Foundation Trust, London, UK

(Chamberlain et al. 2007). However, the dopaminergic action of the drug may not be relevant to behavioural modulation as direct dopaminergic augmentation with L-DOPA has no effect on the task performance (Obeso et al. 2011), strengthening the rationale for the role of noradrenergic transmission in response inhibition (eg., Kehagia et al. 2014; Robbins and Kehagia 2017). In fact, noradrenergic restoration might be a promising clinical strategy in ameliorating some non-motor symptoms in PD including impulsivity (O'Callaghan et al. 2020; Rae et al. 2016) consistent with the early and profound degeneration of the locus coeruleus (LC) in the disease, whereas the underlying neural mechanism of the drug effect is still elusive.

One of the major difficulties in synthesising the neural responses to ATO in response inhibition arises from the recognised confound of attentional capture present on stop trials, which are intended to index inhibition: the conventional stop versus go contrast in functional MRI studies is confounded by the difference of trial frequency between two task conditions, and further complicates the determination of ATO effects on inhibitory control. To disentangle inhibition from attention, one study (Sharp et al. 2010) included a continue signal matching the frequency and temporal profile of stop stimuli as a more appropriate contrast condition suited to neuroimaging. Response inhibition indexed by the more selective stop versus continue contrast revealed enhanced blood oxygenation level-dependent (BOLD) signal over pre-supplementary area (pre-SMA) during response slowing and cancellation. In contrast, the critical role of right inferior frontal cortex implicated by conventional SST in stopping action was not observed using the continue baseline. Other studies directly addressing the role of the rIFC have also linked it to attentional control rather than inhibition (Erika-Florence et al. 2014; Hampshire 2015), a functional dissociation which was further validated in primates using a similar paradigm (Xu et al. 2017).

The second major source of the contention surrounding the effects of ATO is the inconsistent involvement and functional heterogeneity of the right inferior frontal cortex (rIFC) during inhibitory control (Aron et al. 2015; Hampshire and Sharp 2015). The gyrus (rIFG) and its frontostriatal interactions have been identified as the locus of this drug effect by functional magnetic resonance imaging (fMRI) studies (Borchert et al. 2016; Chamberlain et al. 2009; Rae et al. 2016). However, one independent meta-analysis (Swick et al. 2011) pinpointed the neighbouring anterior insula (AI) in classic SST, but reported inconsistent involvement of the rIFG. Another quantitative meta-analysis (Levy and Wagner 2011) on the classic stop–go contrast highlighted broader control of the right inferior frontal junction (rIFJ) over both motor inhibition and attention reorientation. In consistent with the findings in meta-analyses, using multiple baselines isolating inhibition from attention, a functional dorsal–ventral dissociation was found between the salience-driven rIFJ and the rIFG/AI linked to action programming (Sebastian et al. 2016).

The current neuroimaging study addressed these issues directly, to identify brain regions that respond to ATO during response inhibition unconfounded by attentional capture, and to parse the drug effects over the functionally inhomogeneous rIFC in inhibitory control. We implemented a modified SST with attentional capture in a healthy older cohort with an age range matching the typical onset of neurodegenerative disorders to further understand effects of the drug on inhibition in the healthy ageing brain. We hypothesised that behavioural inhibition and associated brain regional activity will be modulated by atomoxetine. Moreover, the LC integrity plays an important role in cognitive reserve for healthy older adults (Mather and Harley 2016) and may predict drug response (O'Callaghan et al. 2020). LC integrity as measured by neuromelanin (NM)-sensitive MRI in vivo can be used to index the regional density of functioning noradrenergic neurons (Clewett et al. 2016; Wilson et al. 2013; Ye et al. 2021), which has been validated by histologic evidence (Keren et al. 2015). Therefore, whether the effect of ATO is dependent on individual variations of LC integrity was investigated. To elucidate these effects further, we focus on (i) the imaging contrast unconfounded by attentional capture, (ii) functional dissociations within the rIFC and (iii) the role of LC signal variation in mediating the drug effects.

Materials and methods

Participants

Nineteen healthy, right-handed male and female participants aged between 45 and 75 years were included in this study following successful screening by interview, history and examination conducted by a study clinician. All participants gave written informed consent. The ethics was approved by the King's College London's Psychiatry, Nursing and Midwifery Research Ethics Committee (HR-15/16–1964). The exclusion criteria were history of psychiatric or neurological disorders; concurrent medication that interacts with the action of the drug; medical conditions that affect hepatic, renal or gastrointestinal functions; cardiac disorders or uncontrolled hypertension; failure of drug of abuse; excessive use of nicotine ($>=5$ cigarettes/day), caffeine ($>=400$ mg/day) and alcohol ($>=28$ units/week); mini-mental state examination (MMSE) score <25; or any MRI contraindications. All participants completed the modified stop-signal task while being scanned but one was excluded due to excessive head movement. The current study is based on the remaining 18 completed data sets (7 males, mean age $\pm$ SD: 58 ± 8.3 years, range: 46–70 years).

Experimental design

This study used a randomised, double-blind, placebo-controlled, within-subject, crossover design. Eligible participants were invited for two study sessions where 40 mg of atomoxetine (ATO) was given orally on one session and 25 mg ascorbic acid placebo (PLA) was given on the other, presented in identical capsules. The 40 mg of atomoxetine was selected because it is the initial dose for efficacy prior to the upward titration for the management of inattention in ADHD, showing good tolerability for both patients and healthy participants according to previous studies (Chamberlain et al. 2009; Warren et al. 2017). For each study session, a standard health safety check was conducted, including pre- and post-dosing physical and brief neurological examinations, ECG and blood pressure measurements. Blood samples were taken at two time points: one at 60 min post-dosing and the other immediately after the scan at approximately 180 min post-dosing. The plasma samples were isolated after centrifugation and shipped to Rudolf-Boehm-Institute of Pharmacology and Toxicology at Leipzig University for the determination of ATO's plasma concentration (online resource 1). Participants entered the scanner at 90 min post-dosing in order to maximise the plasma concentration of ATO based on the typical half-life of the drug (Sauer et al. 2005). The mean plasma concentration between two samples was used to approximate the drug plasma level during the scan.

Stop signal task with attentional capture

The current version of SST was derived from previous studies (Pauls et al. 2012; Sharp et al. 2010), with the attentional capture feature added to disentangle attentional control from motor inhibition (Fig. 1). The SST comprised 420 trials. In the go condition (260 trials), participants were instructed to respond to an arrow pointing left or right with a response box. The trial length was set as 1650 ms and the maximum reaction time (RT) allowed in the task was 1400 ms. In the stop condition (80 trials), an unpredictable stop signal, symbolised by a red dot, would appear following the go signal with variable stop signal delays (SSD), where participants were required to inhibit their responses. The SSD started from 150 ms with a stepwise adaptation procedure using the trial-by-trial adjustment by 50 ms based on the cumulative accuracy of stop responses. The range of SSDs was fixed in between 50 and 900 ms. An additional continue signal (80 trials) informed by a green dot was included matching the frequency and the temporal profile of stop signals; the delay for a given continue signal was set to the SSD used in the most recent stop trial. Participants were instructed to make the same responses on continue as on go trials. Participants received training on the task at screening and were reminded of the task rules on both study days before the scanning.

Behavioural analyses

For each visit, mean RTs of go, continue and failed stop trials were calculated, and the accuracy of go, continue and stop trials was counted. The estimation of the stop-signal reaction time (SSRT) was based on the *integration method*

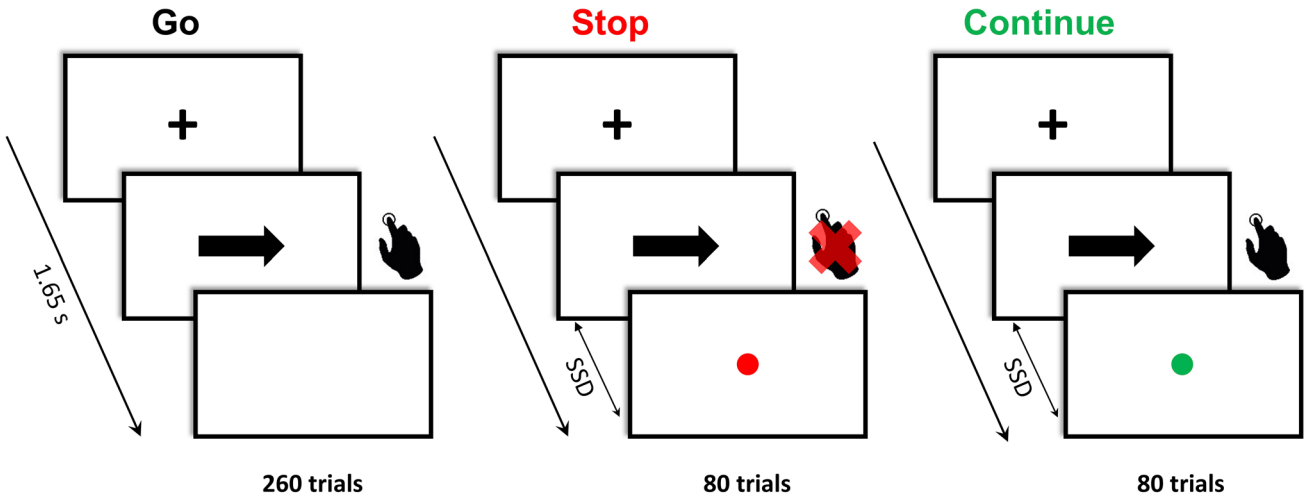

Fig. 1 Stop signal task with three types of trials (Go, Stop and Continue). The inter-trial interval was 1650 ms. Sixty-two percent trials contained Go stimuli for 300 ms. Nineteen percent of the trials included a stop signal (red dot) with varied SSDs as a function of outright stopping frequency. The remaining 19% trials were continue trials, serving to control for attentional capture with the same SSD of the preceding stop trial

(Verbruggen and Logan 2009). This method was selected because it is less susceptible to the skewness of the go RT distribution which might be affected by ageing. According to the recommendations in a recent consensus guide (Verbruggen et al. 2019), omitted go responses were replaced with the maximum RT to form a go distribution in combination with all go trials with a response (including incorrect and premature go responses). This variant of the classic integration method provides a less biased and more reliable estimate on the SSRT. The SSRT was therefore estimated by subtracting the mean stop signal delays from the *n*th RT, where *n* is determined by multiplying the number of go RTs in a full distribution by the overall probability of responding [*p*(respond|signal)].

MRI data acquisition

The MRI data were acquired using a 3.0 Tesla MR750 GE system (General Electric) with a 32-channel head coil. At each scanning session, 383 functional images were acquired during the SST (TR = 2000 ms, TE = 30 ms, Flip Angle = 75°, slice thickness = 3 mm with 0.3 mm gap, FoV = 240 mm, matrix = 64 × 64, in plane resolution = 3 × 3 mm). A high resolution structural MPRAGE image was acquired on the first scanning session (TR = 7.3 ms, TE = 3 ms, TI = 400 ms, Flip Angle = 11°, FoV = 270 mm, matrix = 256 × 256, in plane resolution = 1.2 × 1.2 mm). A 2D T1-weighted turbo spin echo (TSE) sequence was additionally acquired on the second visit for LC localisation and signal quantification. Ten axial high-resolution T1-TSE images were positioned perpendicular to the long axis of the brainstem with acquisition parameters as follows: TR = 600 ms, TE = 21.2 ms, flip angle = 125°; FoV = 220 mm, 2.5 mm slice thickness with 1 mm gap, matrix = 512 × 320, in plane resolution = 0.43 × 0.43 mm.

Image processing and modelling

The functional imaging data were processed using SPM 12 (v6906). Functional volumes were slice-time corrected, realigned and co-registered with the T1-weighted images. The structural data were segmented into three different tissue types (grey matter, white matter and cerebrospinal fluid) which were used to create a group-specific anatomical template using DARTEL (Ashburner 2007). This step produced deformation flow field files which were used to normalise the functional data to the MNI template. An 8 mm FWHM Gaussian kernel was selected for spatial smoothing.

Task events were modelled in a general linear model (GLM), including 4 regressors of interest: correct go trials (GO), correct continue trials (CC), successful stop trials (SS) and failed stop trials (FS). Incorrect go and continue trials were modelled separately as nuisance regressors. For events with recorded responses (GO, CC and FS), the trial durations were modelled with corresponding RTs as such duration modulation captures BOLD responses more reliably and reduces false positives in decision-making tasks (Grinband et al. 2008). The SSD for a successful stop trial was selected as the SS duration in line with previous studies (Sharp et al. 2010). Other trials with no recorded RTs were modelled using the fixed function with the total trial length. A 24-parameter model was used for modelling movement artefacts. All regressors were convolved with a canonical hemodynamic response function. Continue trials were used as the primary baseline for the SS and FS trials (SS > CC, FS > CC) given the control they provide for trial frequency. CC > GO contrast was used to estimate the attention-related processing of the infrequent stimuli. The contrasts traditionally used for indicating inhibitory control in previous studies were also examined (SS > GO, FS > GO).

ROI analyses

To determine whether the effects of ATO in response inhibition are dependent on contrast differences, a priori defined frontal and parietal regions of interest (ROIs) were selected from an SST study incorporating the attentional capture baseline. Five spherical ROIs were created (5 mm radius) using the coordinates reported in Sharp et al. (2010), including lateral (x = 20, y = 6, z = 62) and medial (x = 12, y = 12, z = 58) pre-SMA identified in their SS > CC contrast, the rIFG (x = 44, y = 18, z = 16) and right supramarginal gyrus (SMG: x = 68, y = -42, z = 22) in the SS > GO contrast and anterior cingulate (ACC: x = 2, y = 24, z = 24) in the FS > CC contrast. Furthermore, multiple regions within or close to the rIFC were defined to address the functional heterogeneity of the structure in the current paradigm. These definitions entailed the rIFG reported in Sharp et al. (2010), and the functionally dissociable rIFJ (x = 45, y = 8, z = 25) and rIFG/AI (x = 42, y = 20, z = − 5) identified in Sebastian et al. (2016) as two extra regions located at the boundaries of the rIFC. These ROIs were subsequently used to extract the mean regional parameter estimates from individual contrasts representing inhibitory (SS > CC) and attentional (CC > GO) elements of the task. The confounded stop contrast used in previous studies (SS > GO) was also examined. Whole brain voxel-wise analyses were also performed for the comparison with results from ROI analyses (online resource 3).

In vivo assessment of LC integrity

T1-TSE images were firstly corrected for spatial intensity inhomogeneity using FAST in FSL (Fig. 4A). The peak-intensity detection was selected for LC segmentation because this approach is specific to LC neurons and independent of anatomical boundaries (Clewett et al. 2016;

Keren et al. 2009). The bilateral LC were defined using a cross of 3 voxel width and height to capture the in-plane LC distribution ranging ~ 1.2 mm, centred on the voxel with peak intensity on each side. A circular reference region in the dorsal pontine area was selected as the reference region for signal normalisation (5 voxels radius). The mean (I_{REF}) and standard deviation (I_{SD}) of signal intensity for the reference region and the mean signal intensity for LC ROIs (I_{LC}) collapsed across both hemispheres were calculated. The contrast-to-noise ratio (CNR) was calculated as: $CNR = (I_{LC\_} I_{REF}) / SD_{REF.}$

Statistical models

Statistical analyses were performed using JASP (v0.11.1). Behavioural results were subjected to repeated measures ANOVAs with drug (ATO and PLA) as the within-subject factor and drug order (ATO was given on the 1st or 2nd session) as the between-subject factor. The extracted beta estimates for ROIs were subjected to a repeated measures ANOVA with region, contrast and drug as within-subject factors and drug order as the between-subject factor. Greenhouse–Geisser correction was applied when necessary. Post hoc tests for each ROI were also performed to confirm the specific drug modulation with the Holm correction for multiple testing.

A linear regression model was used to examine potential predictors for the drug responsiveness. The difference score of SSRT (ΔSSRT, PLA-ATO) was calculated as the primary behavioural index for the drug effect on response inhibition. Potential predictors for ΔSSRT were examined separately as well as in a holistic model with age, ATO plasma concentration and LC CNR. The same model was applied on drug-induced changes of regional neural activity specifically in outright stopping using the SS > CC contrast.

Results

Demographic and physiological results

The demographic and individual LC CNR results are summarised in online resource 2. There was no gender difference in the LC CNR ($t(1,16) = 1.34$, $p = 0.2$). The mean signal intensity in the selected reference region did not correlate with age (Spearman rho = 0.006, $p = 0.98$), suggesting that the dorsal pontine area is an appropriate baseline measure. The mean drug plasma level across pre- and post-dosing measures varied between subjects (range: 80.4–743.3 ng/ml). Drug concentration decreased from the first to the second plasma sample in twelve subjects and increased in six.

Behavioural results

Task performance on ATO and PLA is summarised in Table 1. There was no main effect of drug on any RT or accuracy measurement, but the drug effect significantly interacted with administration order for go RTs ($F(1,16) = 17.48$, $p < 0.001$), continue RTs ($F(1,16) = 8.1$, $p = 0.013$) and accuracy on continue trials ($F(1,16) = 7.47$, $p = 0.015$). Compared to PLA, ATO prolonged both go and continue responses when administered on the second session ($p = 0.01$ for go RTs; $p = 0.03$ for continue RTs), whereas faster responses for go trials ($p = 0.01$) and more accurate continue responses ($p = 0.03$) were observed with ATO on the first session. In sum, ATO had no effect on the SSRT and stop accuracy in this group of older healthy participants. Age and ATO plasma level had no significant modulating effects on performance.

Table 1 Behavioural results for RTs and percentage accuracy (mean ± SEM)

Trial type	ATO first ($N = 9$)*			PLA first ($N = 9$)**		
	ATO	PLA	Stats†	ATO	PLA	Stats†
Go RT (ms)	971 ± 48	1029 ± 41	*p = 0.01*	1004 ± 62	927 ± 63	*p = 0.01*
Continue RT (ms)	1042 ± 32	1084 ± 18	*n.s*	1028 ± 52	958 ± 51	*p = 0.03*
Go accuracy (%)	86.0 ± 3.4	85.4 ± 3.4	*n.s*	84.9 ± 5.1	85.5 ± 3.8	*n.s*
Continue accuracy (%)	71.9 ± 6.1	64.0 ± 7.8	*p = 0.03*	69.0 ± 8.2	73.1 ± 7.2	*n.s*
Stop accuracy (%)	51.8 ± 0.9	52.9 ± 0.6	*n.s*	57.5 ± 3.1	51.7 ± 1.2	*n.s*
SSRT (ms)	289 ± 21	304 ± 31	*n.s*	284 ± 24	314 ± 23	*n.s*

The mean RTs for go, continue responses and SSRTs and accuracy on go, continue and stop trials are summarised (±SEM)

*Randomisation type 1: ATO was given on the first study session

**Randomisation type 2: ATO was given on the second study session

†Statistical results for the main effect of drug separated by drug order

n.s. not significant

Neuroimaging results

Results for ROI analyses are presented in Fig. 2. We replicated previous findings on the cortical effects of ATO on response inhibition: there were a main effect of drug ($F(1,17) = 6.17$, $p = 0.02$) and specific drug effects on the rIFG ($p = 0.03$), ACC ($p = 0.04$) and SMG ($p = 0.03$), respectively, examined in post hoc tests. However, when attentional processing is controlled for in the SS > CC contrast, a different drug-related cortical mechanism of inhibitory control emerged. Although the main effect of ATO was obtained (drug: ($F(1,17) = 7.26$, $p = 0.015$), post hoc tests revealed that the drug effect during outright stopping was only seen in lateral pre-SMA ($p = 0.042$) and right SMG ($p = 0.04$). There was no drug effect ($F < 1$) or drug × region interaction ($F(4,14) = 1.5$, $p = 0.23$) for the CC > GO contrast, confirming that attentional processing of frequency information is not modulated by ATO. Including drug order as the between-subject factor had no effect on the results of ROI-based analyses. These findings were also replicated in the whole brain analyses (online resource 4–7).

Moreover, to rule out the potential vascular confound of the drug effect on BOLD responses, peripheral blood pressures (BP) and whole-brain voxelwise signal changes induced via CO2-modulated vasodilation in a breath-hold task were both compared between drug and placebo conditions (online resource 8 & 9). There was no effect of ATO in changing BP ($t(17) < 1$ for both systolic and diastolic BPs) or in modulating BOLD signals during breath-hold (Figure S3), suggesting that the drug effect on the neural responses is unlikely to be driven by cerebrovascular reactivity.

ROI analyses with subdivisions of the rIFC revealed a contrast × region interaction in response to ATO modulation ($F(4,13) = 6.819$, $p = 0.007$). As shown in Fig. 3, post hoc tests revealed that the rIFJ was subject to drug modulation irrespective of baseline selection ($p = 0.043$ for SS > CC

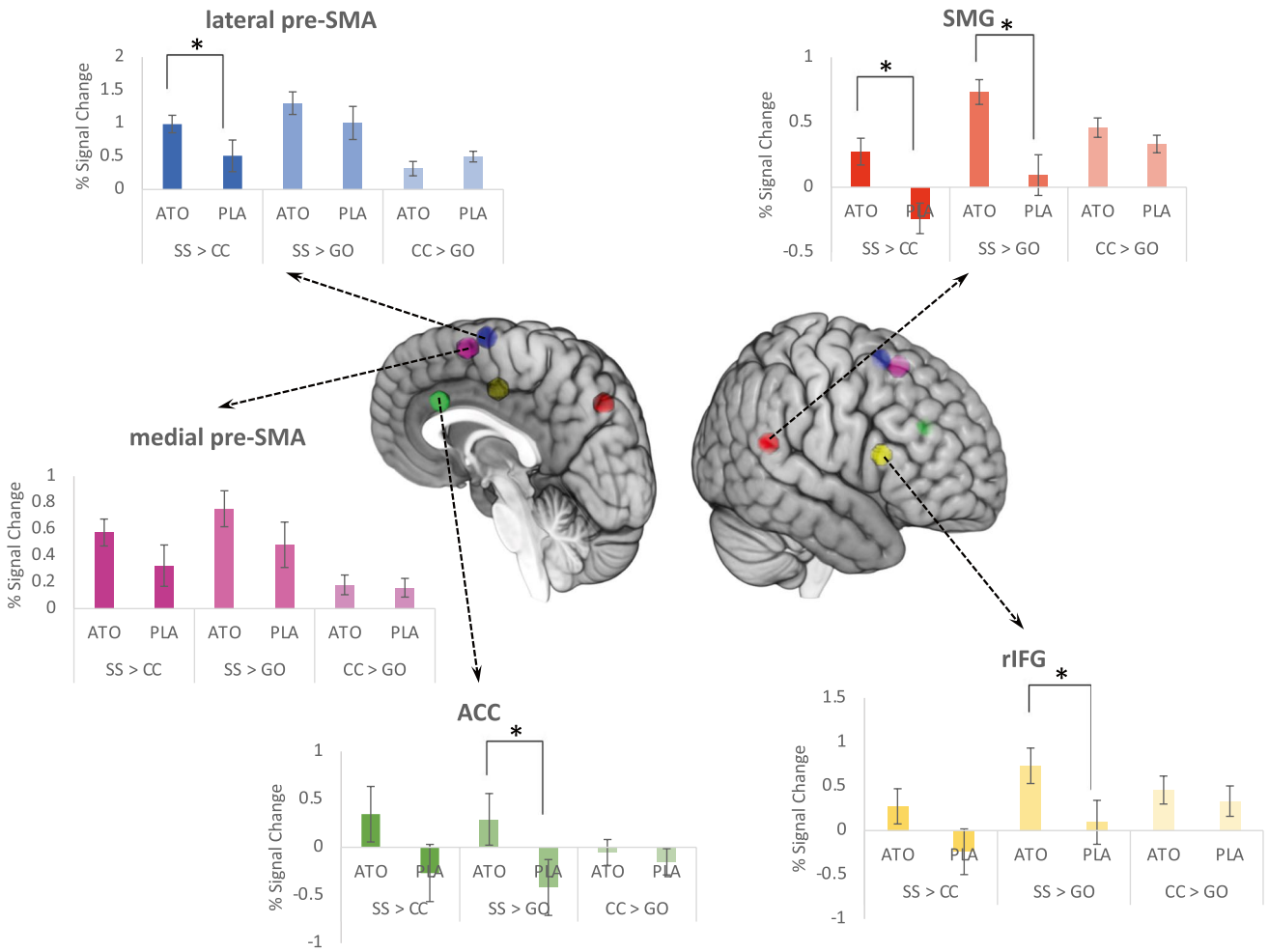

Fig. 2 Percentage signal changes in a priori defined ROIs (blue: lateral/medial pre-SMA, red: SMG, yellow: rIFG, pink: medial pre-SMA, green: ACC) for the Stop versus Continue (SS > CC), Stop versus Go (SS > GO) and Continue versus Go (CC > GO) contrasts (* $p_{holm} < 0.05$, error bars represent SEM)

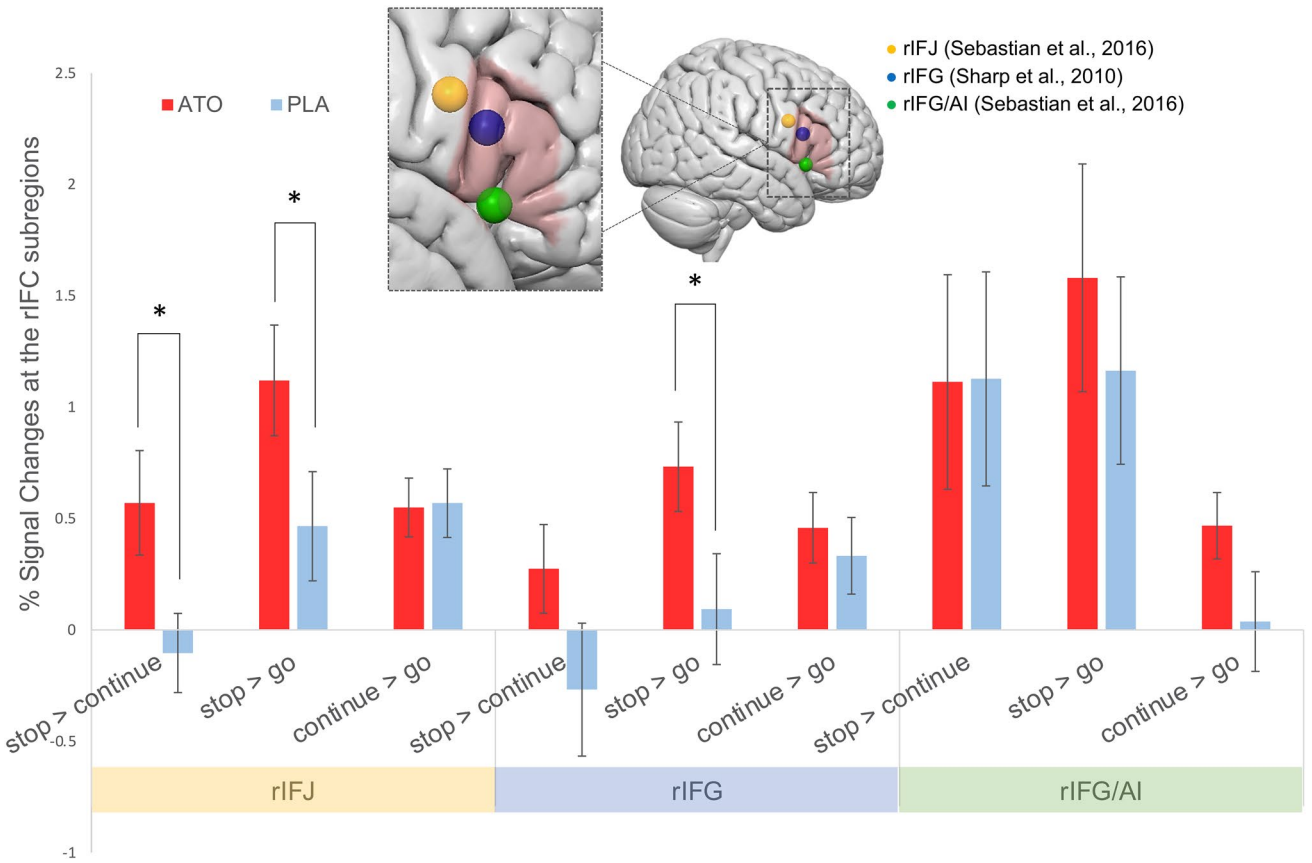

Fig. 3 The effects of ATO on subregions of the rIFC for SS > CC, SS > GO and CC > GO contrasts (* indicates $p_{holm} < 0.05$ in post-hoc tests). Locations of the rIFJ, rIFG and rIFG/AI are overlaid onto a 3D rendered brain template for visualisation. The pink area represents the anatomical definition of the rIFG (pars opercularis and pars triangularis) derived from the Harvard–Oxford atlas

contrast; $p = 0.05$ for SS > GO contrast). In contrast, the drug effect in the rIFG can be observed using the classic SS > GO contrast confounded by attentional capture ($p = 0.03$), but not for the SS > CC contrast ($p = 0.123$). No contrast has revealed any drug modulation on rIFG/AI. ATO had no effect on any rIFC subregions in the CC > GO contrast. Drug order had no effect on these findings.

LC integrity and drug effects.

Next, we focused on testing the role of LC integrity in modulating behavioural and neural effects of ATO in response inhibition where the LC was measured in vivo using neuromelanin-sensitive sequence (Fig. 4A). A quadratic relationship was detected between LC CNR and ΔSSRT (Fig. 4B, $R^2 = 0.411$, $F(2,17) = 5.24$, $p_{model} = 0.019$, $\beta_{LC} = 4.05$, $p = 0.006$, $\beta_{LC2} = -3.98$, $p = 0.006$) which remained significant when age and ATO plasma level were additionally included in the model ($R^2 = 0.377$, $F(4,13) = 3.57$, $p_{model} = 0.035$, $\beta_{LC} = 4.44$, $p = 0.003$, $\beta_{LC2} = -4.42$, $p = 0.003$). Moderate level of LC CNR was linked with ATO-induced SSRT reduction, whereas higher or lower LC CNR was associated with increased SSRT after a single dose of ATO. We also explored the role of LC integrity in mediating the drug effect on the pre-SMA and the SMG, the two brain regions whose neural activities were enhanced by ATO during outright stopping (SS > CC). The exploratory analyses revealed a significant linear relationship between ATO-related signal change in the SMG and LC CNR for the SS > CC contrast (Fig. 4C, $R^2 = 0.274$, $F(1,16) = 6.04$, $\beta_{LC} = 0.52$, $p = 0.026$). This relationship remained significant after including age and plasma level of ATO as covariates ($R^2 = 0.422$, $F(3,14) = 3.411$, $\beta_{LC} = 0.54$, $p = 0.023$). The ATO effect in the pre-SMA was not mediated by LC integrity ($F(2,17) = 1.44$, $\beta_{LC} = 0.29$, $p = 0.25$).

Discussion

In this study, the effect of ATO on response inhibition was revisited with a modified version of the SST that controls for attentional capture. This experimental manipulation was adopted to disentangle the neural mechanisms of the drug that are specific to inhibitory control by introducing a more effective comparison condition in the fMRI contrast that models stopping per se. For this contrast, we obtained

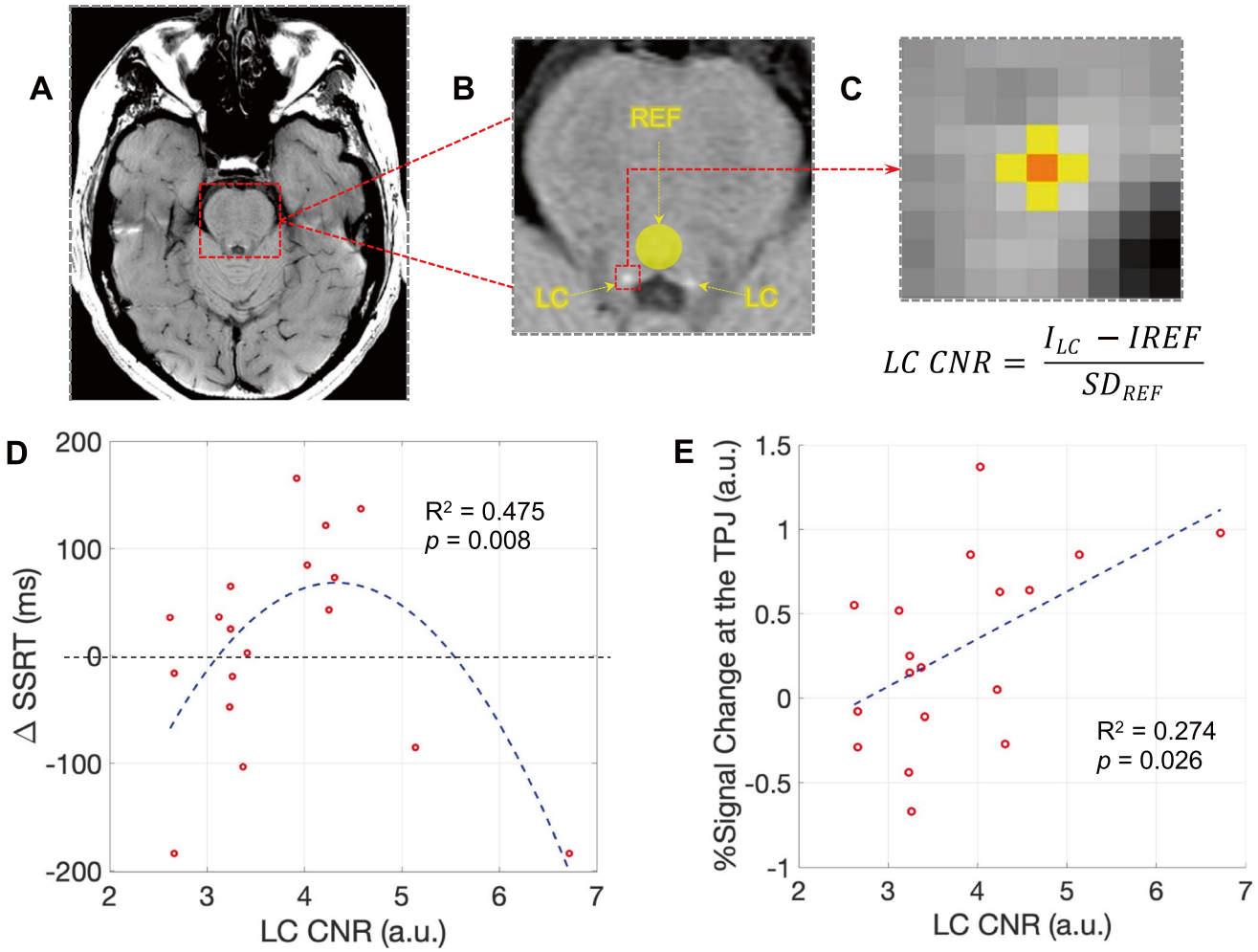

Fig. 4 LC CNR calculation and correlations with behavioural and imaging results. **A** Locations of LC bilaterally and reference dorsal pontine region with the distribution of the LC ROI used for the CNR extraction. **B** Relationship between LC CNR and ATO-induced SSRT changes. **C** Relationship between LC CNR and signal changes at the SMG (stop > continue)

BOLD signal increase over pre-SMA and SMG with a single dose of ATO. The drug also modulated the rIFJ, instead of the rIFG, during inhibition. Furthermore, signal intensity in the LC, the main source of cortical NA, correlated with signal change variability over SMG, further supporting the role of LC-integrity on response inhibition.

Previous studies have highlighted the importance of the pre-SMA in motor inhibition (Chen et al. 2010; Obeso et al. 2013), which ATO modulates during outright stopping. In the current study, a more selective control condition in the form of continue trials was used to match the frequency and temporal profile of critical stop signals. When we specifically interrogated the subregions of medial and lateral pre-SMA, using predefined regions, the effect of ATO was restricted to the lateral pre-SMA. The lateral pre-SMA is functionally distinguishable from the more medial and rostral subregions, which may be more involved in the process of response conflict (Sharp et al. 2010). In line with the proposed functional specificity of the pre-SMA in motor control, imaging studies in PD patients have shown decreased activation in this region (Lindenbach and Bishop 2013), and diminished cortical and subcortical connectivity during the SST, which can be ameliorated by a single dose of ATO (Rae et al. 2016).

Compared to previous studies emphasising a dedicated and unified role of the rIFC during response inhibition, our results describe a dissociable and heterogeneous functional mapping of this structure whereby the observable drug effects on the rIFC depends on the choice of rIFC subregion for a given contrast. In comparison to the go baseline, the increased ventrolateral rIFC activation on ATO seen in our study echoes findings in healthy adults and patients with PD (Chamberlain et al. 2009; Rae et al. 2016). However, employing the CC > GO contrast to index attentional reorientation revealed comparable effect of ATO and PLA over the rIFG, suggesting that the effect of ATO does not in fact extend to this non-selective

process. Furthermore, our findings of varied cortical effects following ATO administration mirror the dorsal-to-ventral functional dissociation in the rIFC. Specifically, a baseline-independent effect of drug modulation was observed only for the dorsally located rIFJ, whereas the ventral rIFG/AI showed no response to the drug (Fig. 3). In the stop task, the role of the rIFJ can be dissociated from that of the rIFG/AI when controlling for attentional capture, where the latter more specifically contributes to action plan updating and the implementation of cognitive control (Cai et al. 2014; Sebastian et al. 2016; Verbruggen et al. 2010). Unlike the rIFG, IFJ activation has been consistently reported in tasks relying on various cognitive abilities such as in task switching (Derrfuss et al. 2005), providing a more domain-general control function (Levy and Wagner 2011). The IFJ has also been proposed to mediate interactive inputs from neighbouring structures which manipulate stimulus–response mapping and working memory (Brass et al. 2005). In line with this, we propose that by modulating the rIFJ, ATO promotes response inhibition via an integrative mechanism involving top-down control over multiple, critical, task demand dictated functions.

The SMG, which is also modulated by ATO during stopping irrespective of the comparison condition, is another candidate region contributing to functional integration during response inhibition. In the whole-brain analysis, the cortical extent of this cluster coincides with the anatomical location of the temporoparietal junction (TPJ), another key node within the ventral attention network (Corbetta et al. 2008). Neural activity in the TPJ is suppressed during focused attention by direct cortical or indirect subcortical circuits (Shulman et al. 2003). Consistently with more recent findings highlighting a domain-general role of the TPJ (Geng and Vossel 2013), the observed effects of ATO over this region signify facilitation over the detection of behaviourally critical, yet infrequent stop signals.

While the inclusion of continue stimuli in the current version of the task has been widely used to isolate motor inhibition and detection of the stop signal, this task design has been criticised for response slowing on continue trials which might complicate the interpretation of our results. Recent studies have shown that infrequent stimuli in the stop-signal task can elicit residual brain activations similar to stop-related neural signatures, the degree of which predicts the speed of action slowing after infrequent events (Waller et al. 2019). We acknowledge that this type of slowing might reflect a 'brake' mechanism in reactive motor inhibition where the action stopping is gradually achieved in response to behaviourally relevant stimuli (Aron et al. 2015; Wessel and Aron 2017). However, this inhibition-like response slowing effect on continue trials does not compromise its validity as a frequency-controlled baseline: when contrasting stop responses to a stringent baseline encompassing continue trials with potential action slowing features, we still observed brain activations that are typically involved in motoric inhibition (Fig. 2) even when the drug modulation was absent. The distinctive activation patterns revealed in SS > CC, SS > GO and CC > GO contrasts in the current study mimicked the same functional dissociation between motor control brain regions and rIFC subregions in an fMRI and neurophysiological study in humans and primates (Xu et al. 2017) which showed that ventral rIFC specifically encodes the context of the stimulus–response mapping, indirectly contributing to inhibitory control rather than being directly responsible for behavioural inhibition. Moreover, although attentional features were explicitly controlled in the current task design, the mechanism underpinning the neuromodulatory effect of atomoxetine in response inhibition cannot wholly exclude a drug effect on attention-related cognitive processing: the two brain regions whose neural activities were altered, SMG/TPJ and rIFJ, subserve integration that mediates multifactorial cognitive control, recruiting cortical and subcortical regions in the attention network.

Our findings are in line with current theories of noradrenergic function in cognition (Aston-Jones and Cohen 2005; Dayan and Yu 2006) where a low dose of ATO may enhance the phasic-to-tonic ratio of LC neuronal activity (Bari and Aston-Jones 2013). This drug action on the LC distally facilitates the processing of task-relevant, resource-demanding events at the cortical level, such as the SMG/TPJ area (Kahnt and Tobler 2013). This is supported by the positive linear relationship between the LC CNR and the drug-induced signal changes in the right SMG, and behaviourally a LC CNR-dependant drug-related SSRT changes. However, this evidence must be considered exploratory before it is validated in a larger study. Thus, NA represents a common neurochemical denominator for both attention and inhibition (Robbins and Kehagia 2017), and the LC represents a putative anatomical source of this modulation (Bari and Aston-Jones 2013). The LC contrast can reliably index the structural integrity of the LC-NA system as neuromelanin-sensitive MRI has been histologically validated (Keren et al. 2015). The application of this in vivo imaging assessment of the LC-NA system might be valuable in neurodegenerative disorders for early detection and monitoring of evolving pathology (Betts et al. 2019) and could support personalised medicine strategies (O'Callaghan et al. 2020).

Several limitations need to be addressed in future studies. Behaviour was not altered in our group by the drug effect, though this could reflect a ceiling effect, not readily amenable to improvement as seen on tasks with limited age-related decrements (Rey-Mermet and Gade 2018). The dose may also have been insufficient to alter performance. Nevertheless, it has been argued that imaging effects in the absence of behavioural change effect on task performance allow for more precise modelling of the BOLD signal response without a differential confound of error trials between conditions (Murphy

and Garavan 2004). In addition, the sample size in the current study might be sufficient for detecting a modulatory effect of atomoxetine on some brain regions at a lower dose, whereas the involvement of other brain regions less responsive to the drug might be determined using bigger samples and/or higher doses in future studies. Moreover, sensitivity and reliability of LC measurement can be improved upon using more advanced sequences and at higher magnetic field strengths (Priovoulos et al. 2018; Ye et al. 2021) as the LC is a small, narrow, elongated structure on the rostrocaudal axis of the pons. A magnetisation transfer-weighted sequence combined with ultra-high field 7 T MRI is sufficient to provide submillimetre resolution for imaging the structure which allows more accurate and sensitive investigation on the effect of LC integrity in mediating noradrenergic modulation in response inhibition (O'Callaghan et al. 2021; Ye et al. 2021).

The results of this study point to a model of noradrenergic modulation of inhibition involving critical nodes of the ventral attentional network (TPJ, rIFJ) along with the pre-SMA and its enhanced connectivity to the STN. From a methodological perspective, combining ATO with a modified SST, including controls for attentional capture, illustrates the importance and utility of baseline conditions in psychopharmacological imaging studies as a means of unconfounding cognition, and elucidating its underlying neurochemistry. Moreover, we have demonstrated that employing neuromelanin-sensitive MRI to target the LC is a promising step toward more holistic models of brain function and pharmacological modulation, with significant implications in neurodegenerative diseases.

Supplementary Information The online version contains supplementary material available at https://doi.org/10.1007/s00213-021-05998-2.

Acknowledgements We thank all the study participants for their time and commitment. We gratefully acknowledge S. Stephensen, V. Kotoula and P. Selvaggi for assistance with data collection; D. Lythgoe for the neuromelanin-sensitive sequence development.

Funding This study was funded from departmental sources.

Declarations

Conflict of interest The authors declare no competing financial interests. R. Y. is grateful for support from the China Scholarship Council (CSC). A. A. K. was supported by the King's College London and a Fellowship from the Foulkes Foundation during her training in medicine. M. A. M was partly supported by the National Institute for Health Research Biomedical Research Centre at South London and the Maudsley NHS Foundation Trust and King's College London.

References

Aron AR, Cai W, Badre D, Robbins TW (2015) Evidence supports specific braking function for inferior PFC. Trends Cogn Sci 19:711–712

Ashburner J (2007) A fast diffeomorphic image registration algorithm. Neuroimage 38:95–113

Aston-Jones G, Cohen JD (2005) An integrative theory of locus coeruleus-norepinephrine function: adaptive gain and optimal performance. Annu Rev Neurosci 28:403–450

Bari A, Aston-Jones G (2013) Atomoxetine modulates spontaneous and sensory-evoked discharge of locus coeruleus noradrenergic neurons. Neuropharmacology 64:53–64

Bari A, Eagle DM, Mar AC, Robinson ESJ, Robbins TW (2009) Dissociable effects of noradrenaline, dopamine, and serotonin uptake blockade on stop task performance in rats. Psychopharmacology 205:273–283

Betts MJ, Kirilina E, Otaduy MCG, Ivanov D, Acosta-Cabronero J, Callaghan MF, Lambert C, Cardenas-Blanco A, Pine K, Passamonti L, Loane C, Keuken MC, Trujillo P, Lusebrink F, Mattern H, Liu KY, Priovoulos N, Fliessbach K, Dahl MJ, Maass A, Madelung CF, Meder D, Ehrenberg AJ, Speck O, Weiskopf N, Dolan R, Inglis B, Tosun D, Morawski M, Zucca FA, Siebner HR, Mather M, Uludag K, Heinsen H, Poser BA, Howard R, Zecca L, Rowe JB, Grinberg LT, Jacobs HIL, Duzel E, Hammerer D (2019) Locus coeruleus imaging as a biomarker for noradrenergic dysfunction in neurodegenerative diseases. Brain 142:2558–2571

Borchert RJ, Rittman T, Passamonti L, Ye Z, Sami S, Jones SP, Nombela C, Rodriguez PV, Vatansever D, Rae CL, Hughes LE, Robbins TW, Rowe JB (2016) Atomoxetine enhances connectivity of prefrontal networks in Parkinson's disease (vol 41, pg 2171, 2016). Neuropsychopharmacology 41:2188–2188

Brass M, Derrfuss J, Forstmann B, von Cramon DY (2005) The role of the inferior frontal junction area in cognitive control. Trends Cogn Sci 9:314–316

Bymaster FP, Katner JS, Nelson DL, Hemrick-Luecke SK, Threlkeld PG, Heiligenstein JH, Morin SM, Gehlert DR, Perry KW (2002) Atomoxetine increases extracellular levels of norepinephrine and dopamine in prefrontal cortex of rat: a potential mechanism for efficacy in attention deficit/hyperactivity disorder. Neuropsychopharmacology : Official Publication of the American College of Neuropsychopharmacology 27:699–711

Cai WD, Ryali S, Chen TW, Li CSR, Menon V (2014) Dissociable roles of right inferior frontal cortex and anterior insula in inhibitory control: evidence from intrinsic and task-related functional parcellation, connectivity, and response profile analyses across multiple datasets. J Neurosci 34:14652–14667

Chamberlain SR, Del Campo N, Dowson J, Muller U, Clark L, Robbins TW, Sahakian BJ (2007) Atomoxetine improved response inhibition in adults with attention deficit/hyperactivity disorder. Biol Psychiatry 62:977–984

Chamberlain SR, Hampshire A, Muller U, Rubia K, Del Campo N, Craig K, Regenthal R, Suckling J, Roiser JP, Grant JE, Bullmore ET, Robbins TW, Sahakian BJ (2009) Atomoxetine modulates right inferior frontal activation during inhibitory control: a pharmacological functional magnetic resonance imaging study. Biol Psychiat 65:550–555

Chamberlain SR, Muller U, Blackwell AD, Clark L, Robbins TW, Sahakian BJ (2006) Neurochemical modulation of response inhibition and probabilistic learning in humans. Science 311:861–863

Chen X, Scangos KW, Stuphorn V (2010) Supplementary motor area exerts proactive and reactive control of arm movements. J Neurosci 30:14657–14675

Clewett DV, Lee TH, Greening S, Ponzio A, Margalit E, Mather M (2016) Neuromelanin marks the spot: identifying a locus coeruleus biomarker of cognitive reserve in healthy aging. Neurobiol Aging 37:117–126

Corbetta M, Patel G, Shulman GL (2008) The reorienting system of the human brain: from environment to theory of mind. Neuron 58:306–324

Coxon JP, Goble DJ, Leunissen I, Van Impe A, Wenderoth N, Swinnen SP (2016) Functional brain activation associated with inhibitory control deficits in older adults. Cereb Cortex 26:12–22

Dalley JW, Robbins TW (2017) Fractionating impulsivity: neuropsychiatric implications. Nat Rev Neurosci 18:158–171

Dayan P, Yu AJ (2006) Phasic norepinephrine: a neural interrupt signal for unexpected events. Network 17:335–350

Derrfuss J, Brass M, Neumann J, von Cramon DY (2005) Involvement of the inferior frontal junction in cognitive control: meta-analyses of switching and Stroop studies. Hum Brain Mapp 25:22–34

Erika-Florence M, Leech R, Hampshire A (2014) A functional network perspective on response inhibition and attentional control. Nat Commun 5:4073

Geng JJ, Vossel S (2013) Re-evaluating the role of TPJ in attentional control: contextual updating? Neurosci Biobehav Rev 37:2608–2620

Gilmour G, Arguello A, Bari A, Brown VJ, Carter C, Floresco SB, Jentsch DJ, Tait DS, Young JW, Robbins TW (2013) Measuring the construct of executive control in schizophrenia: Defining and validating translational animal paradigms for discovery research. Neurosci Biobehav Rev 37:2125–2140

Grinband J, Wager TD, Lindquist M, Ferrera VP, Hirsch J (2008) Detection of time-varying signals in event-related fMRI designs. Neuroimage 43:509–520

Hampshire A (2015) Putting the brakes on inhibitory models of frontal lobe function. Neuroimage 113:340–355

Hampshire A, Sharp D (2015) Inferior PFC subregions have broad cognitive roles. Trends Cogn Sci 19:712–713

Kahnt T, Tobler PN (2013) Salience signals in the right temporoparietal junction facilitate value-based decisions. J Neurosci 33:863–869

Kehagia AA, Housden CR, Regenthal R, Barker RA, Muller U, Rowe J, Sahakian BJ, Robbins TW (2014) Targeting impulsivity in Parkinson's disease using atomoxetine. Brain : a journal of neurology 137: 1986-97.

Keren NI, Lozar CT, Harris KC, Morgan PS, Eckert MA (2009) In vivo mapping of the human locus coeruleus. Neuroimage 47:1261–1267

Keren NI, Taheri S, Vazey EM, Morgan PS, Granholm AC, Aston-Jones GS, Eckert MA (2015) Histologic validation of locus coeruleus MRI contrast in post-mortem tissue. Neuroimage.

Levy BJ, Wagner AD (2011) Cognitive control and right ventrolateral prefrontal cortex: reflexive reorienting, motor inhibition, and action updating. Ann N Y Acad Sci 1224:40–62

Lindenbach D, Bishop C (2013) Critical involvement of the motor cortex in the pathophysiology and treatment of Parkinson's disease. Neurosci Biobehav Rev 37:2737–2750

Lipszyc J, Schachar R (2010) Inhibitory control and psychopathology: a meta-analysis of studies using the stop signal task. J Int Neuropsychol Soc 16:1064–1076

Mather M, Harley CW (2016) The locus coeruleus: essential for maintaining cognitive function and the aging brain. Trends Cogn Sci 20:214–226

Murphy K, Garavan H (2004) An empirical investigation into the number of subjects required for an event-related fMRI study. Neuroimage 22:879–885

O'Callaghan C, Hezemans FH, Ye R, Rua C, Jones PS, Murley AG, Holland N, Regenthal R, Tsvetanov K, Wolpe N, Barker R, Williams-Gray C, Robbins T, Passamonti L, Rowe J (2020) Locus coeruleus integrity and the effect of atomoxetine on response inhibition in Parkinson's disease. 2020.09.03.20176800.

O'Callaghan C, Hezemans FH, Ye R, Rua C, Jones PS, Murley AG, Holland N, Regenthal R, Tsvetanov KA, Wolpe N, Barker RA, Williams-Gray CH, Robbins TW, Passamonti L, Rowe JB (2021) Locus coeruleus integrity and the effect of atomoxetine on response inhibition in Parkinson's disease. Brain.

Obeso I, Robles N, Marron EM, Redolar-Ripoll D (2013) Dissociating the role of the pre-SMA in response inhibition and switching: a combined online and offline TMS approach. Front Hum Neurosci 7:150

Obeso I, Wilkinson L, Jahanshahi M (2011) Levodopa medication does not influence motor inhibition or conflict resolution in a conditional stop-signal task in Parkinson's disease. Exp Brain Res 213:435–445

Pauls AM, O'Daly OG, Rubia K, Riedel WJ, Williams SC, Mehta MA (2012) Methylphenidate effects on prefrontal functioning during attentional-capture and response inhibition. Biol Psychiat 72:142–149

Priovoulos N, Jacobs HIL, Ivanov D, Uludag K, Verhey FRJ, Poser BA (2018) High-resolution in vivo imaging of human locus coeruleus by magnetization transfer MRI at 3T and 7T. Neuroimage 168:427–436

Rae CL, Nombela C, Rodriguez PV, Ye Z, Hughes LE, Jones PS, Ham T, Rittman T, Coyle-Gilchrist I, Regenthal R, Sahakian BJ, Barker RA, Robbins TW, Rowe JB (2016) Atomoxetine restores the response inhibition network in Parkinson's disease. Brain : a Journal of Neurology 139:2235–2248

Rey-Mermet A, Gade M (2018) Inhibition in aging: what is preserved? What declines? A meta-analysis. Psychon B Rev 25:1695–1716

Robbins TW, Kehagia AA (2017) The neurochemistry of prefrontal control processes. In: Eigner T (ed) The Wiley Handbook of Cognitive Control. John Wiley and Sons, Chichester, UK

Robinson ES, Eagle DM, Mar AC, Bari A, Banerjee G, Jiang X, Dalley JW, Robbins TW (2008) Similar effects of the selective noradrenaline reuptake inhibitor atomoxetine on three distinct forms of impulsivity in the rat. Neuropsychopharmacology 33:1028–1037

Sauer JM, Ring BJ, Witcher JW (2005) Clinical pharmacokinetics of atomoxetine. Clin Pharmacokinet 44:571–590

Sebastian A, Baldermann C, Feige B, Katzev M, Scheller E, Hellwig B, Lieb K, Weiller C, Tuscher O, Kloppel S (2013) Differential effects of age on subcomponents of response inhibition. Neurobiol Aging 34:2183–2193

Sebastian A, Jung P, Neuhoff J, Wibral M, Fox PT, Lieb K, Fries P, Eickhoff SB, Tuscher O, Mobascher A (2016) Dissociable attentional and inhibitory networks of dorsal and ventral areas of the right inferior frontal cortex: a combined task-specific and coordinate-based meta-analytic fMRI study. Brain Struct Funct 221:1635–1651

Sharp DJ, Bonnelle V, De Boissezon X, Beckmann CF, James SG, Patel MC, Mehta MA (2010) Distinct frontal systems for response inhibition, attentional capture, and error processing. Proc Natl Acad Sci U S A 107:6106–6111

Shulman GL, McAvoy MP, Cowan MC, Astafiev SV, Tansy AP, d'Avossa G, Corbetta M (2003) Quantitative analysis of attention and detection signals during visual search. J Neurophysiol 90:3384–3397

Swick D, Ashley V, Turken U (2011) Are the neural correlates of stopping and not going identical? Quantitative meta-analysis of two response inhibition tasks. Neuroimage 56:1655–1665

Tsvetanov KA, Ye Z, Hughes L, Samu D, Treder MS, Wolpe N, Tyler LK, Rowe JB, Neuroscience CCA (2018) Activity and Connectivity Differences Underlying Inhibitory Control Across the Adult Life Span. J Neurosci 38:7887–7900

Verbruggen F, Aron AR, Band GPH, Beste C, Bissett PG, Brockett AT, Brown JW, Chamberlain SR, Chambers CD, Colonius H, Colzato LS, Corneil BD, Coxon JP, Dupuis A, Eagle DM, Garavan H, Greenhouse I, Heathcote A, Huster RJ, Jahfari S, Kenemans JL, Leunissen I, Li CSR, Logan GD, Matzke D, Morein-Zamir S, Murthy A, Pare M, Poldrack RA, Ridderinkhof KR, Robbins TW, Roesch MR, Rubia K, Schachar RJ, Schall JD, Stock AK, Swann NC, Thakkar KN, van der Molen MW, Vermeylen L, Vink M, Wessel JR, Whelan R, Zandbelt BB, Boehler CN (2019) A

consensus guide to capturing the ability to inhibit actions and impulsive behaviors in the stop-signal task. Elife 8.

Verbruggen F, Aron AR, Stevens MA, Chambers CD (2010) Theta burst stimulation dissociates attention and action updating in human inferior frontal cortex. Proc Natl Acad Sci USA 107:13966–13971

Verbruggen F, Logan GD (2008) Response inhibition in the stop-signal paradigm. Trends Cogn Sci 12:418–424

Verbruggen F, Logan GD (2009) Models of response inhibition in the stop-signal and stop-change paradigms. Neurosci Biobehav Rev 33:647–661

Waller DA, Hazeltine E, Wessel JR (2019) Common neural processes during action-stopping and infrequent stimulus detection: the frontocentral P3 as an index of generic motor inhibition. Int J Psychophysiol.

Warren CM, Wilson RC, van der Wee NJ, Giltay EJ, van Noorden MS, Cohen JD, Nieuwenhuis S (2017) The effect of atomoxetine on random and directed exploration in humans. PloS one 12:e0176034

Wessel JR, Aron AR (2017) On the globality of motor suppression: unexpected events and their influence on behavior and cognition. Neuron 93:259–280

Wilson RS, Nag S, Boyle PA, Hizel LP, Yu L, Buchman AS, Schneider JA, Bennett DA (2013) Neural reserve, neuronal density in the locus ceruleus, and cognitive decline. Neurology 80:1202–1208

Xu KZ, Anderson BA, Emeric EE, Sali AW, Stuphorn V, Yantis S, Courtney SM (2017) Neural basis of cognitive control over movement inhibition: human fMRI and primate electrophysiology evidence. Neuron 96: 1447-+.

Ye R, Rua C, O'Callaghan C, Jones PS, Hezemans FH, Kaalund SS, Tsvetanov KA, Rodgers CT, Williams G, Passamonti L, Rowe JB (2021) An in vivo probabilistic atlas of the human locus coeruleus at ultra-high field. Neuroimage 225:117487